Adaptability of GPS / BDS Broadcast Ionospheric Models to Solar Activity

Na Cheng[1,2], Shuli Song[1]

[1]Shanghai Astronomical Observatory, Chinese Academy of Sciences, Shanghai, China

[2]Graduate School, Chinese Academy of Sciences, Beijing, China

Abstract

The ionospheric delay is one of the main errors for Global Navigation Satellite System (GNSS) signals propagation. It may degrade the accuracy of GNSS signals and affect the performance of GNSS Standard Point Positioning(SPP). For GNSS single frequency users, it can be mitigated by GNSS broadcast ionospheric model. However, the accurate characterization of ionosphere in the current models used in GNSS remains a challenging problem under disturbed ionospheric conditions, such as geomagnetic storms and solar flares.

This study analyzed the adaptability of GPS/BDS broadcast ionospheric models in China and ionospheric total electron content (TEC) anomalies during the high solar activity years 2014-2015.In this work, twelve X-class and M-class large solar flares are investigated and analyzed. It is found that there is the Sudden Increase in Total Electron Content (SITEC) occurred during solar flare. And the effect on accuracy of GPS/BDS ionospheric model is obvious. There is a dramatic variation for GPS/BDS RD values caused by flares. The TEC anomalies and the accuracy of ionospheric models is closely correlated with the flares maximal X-ray flux. It is also related to the position of stations.

Data and Method

Ionospheric TEC measurements

GPS observations from 17 stations of Crustal Movement Observation Network of China （CMONOC） are used to estimate TEC over China. Fig. 1 shows the geographic locations of GPS receiver stations. The increase of TEC and rate of TEC（ROT）during the solar flares are calculated at these stations. The functional model of TEC estimation using GPS can be expressed as follows:

$$TEC=-\frac{1}{40.28}\frac{f_i^2 f_j^2}{f_i^2-f_j^2}(P_j-P_i-(B_j^S-B_i^S)+(B_j^R-B_i^R))$$

$$=-\frac{1}{40.28}\frac{f_i^2 f_j^2}{f_i^2-f_j^2}(\Delta P_{ij}-\Delta B_{ij}^S+\Delta B_{ij}^R)$$

The ROT is computed with TEC data as:

$$ROT=\frac{\Delta TEC}{\Delta t}$$

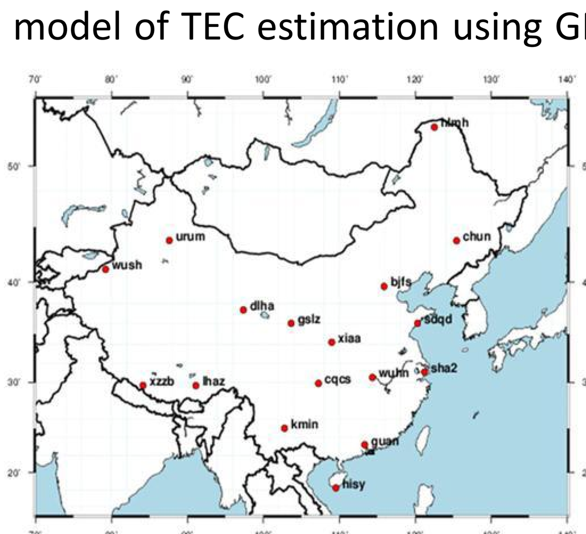

Figure 1. Stations Distribution

GPS/BDS broadcast ionospheric models

Single frequency users need the ionospheric prediction model broadcasted by GNSS satellites to correct the ionospheric delay. BDS and GPS single-frequency positioning ionospheric delay corrections use the different Klobuchar models. The BDS and GPS Klobuchar models have some similarities in both expression and algorithm. The model features are shown in Tab.1. The algorithm of Klobuchar model is expressed as follows:

$$\Delta\tau=\left[D+A\cdot\cos\frac{2\pi(t-T_p)}{P}\right]\cdot MF$$

Table 1. GPS/BDS broadcast ionospheric models features [1,2]

Broadcast ionospheric model	GPS Klobuchar	BDS Klobuchar
Reference frames	Solar-geomagnetic	Geography
Mapping function	$F=1.0+16.0*(0.53-E)^3$	$F=1/\cos z$
Thin-shell Height/km	350	375
Coefficients update period	1day	2hours
Data sources	Global monitoring network	China regional monitoring network

Results and Discussion

In our study, twelve solar flares events took place from 2014 to 2015, with class X and M, were selected to analyze the TEC anomalies and the adaptability of GPS/BDS broadcast ionospheric models over China. Here, the results during a large solar flare is analyzed and shown in detail. The solar flare of class X4.9 occurred on February 25th, 2014, it began at 00:39:00UT and end at 1:03:00UTC. In order to show the effect caused by the solar flare, the TEC and ROT variations at the same time of three days from February 24th to 26th are analyzed. Meanwhile, the increment of ROT, STEC, VTEC at stations are computed by Ten - order polynomial fitting.

TEC anomaly

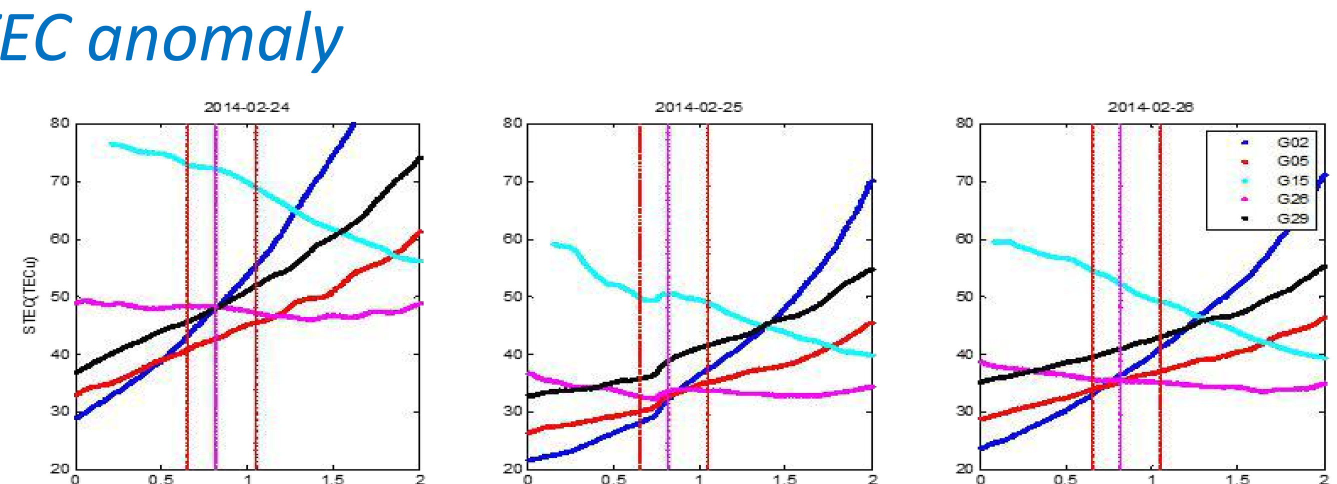

Figure 2. Observed STEC variations during the solar flare at station BJFS

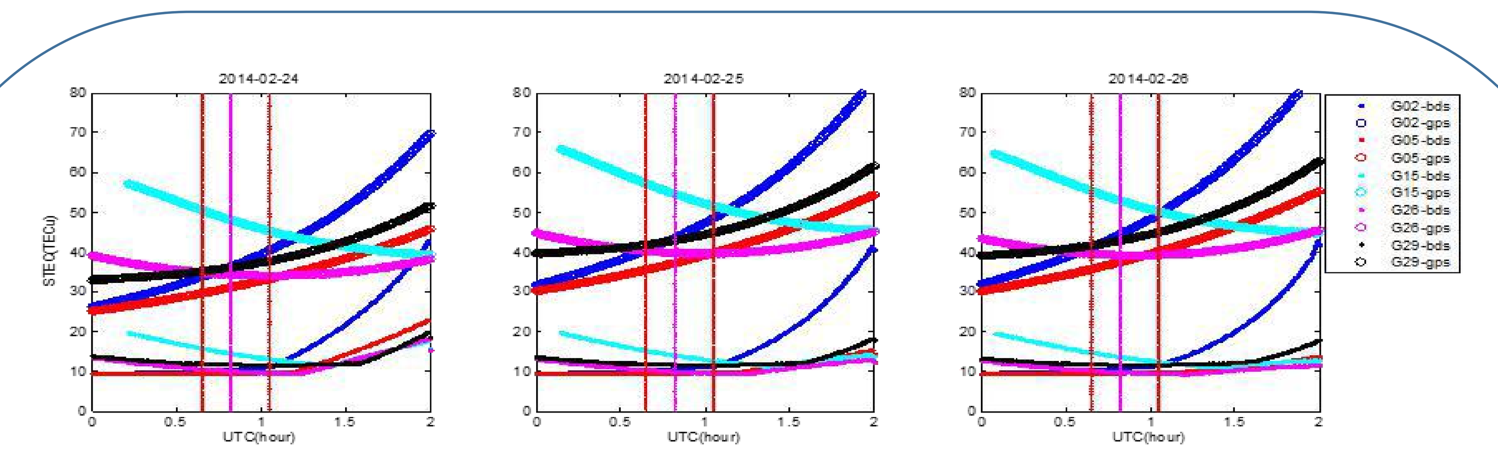

Figure 3. STEC (from GPS/BDS broadcast ionospheric models) during the solar flare at station BJFS

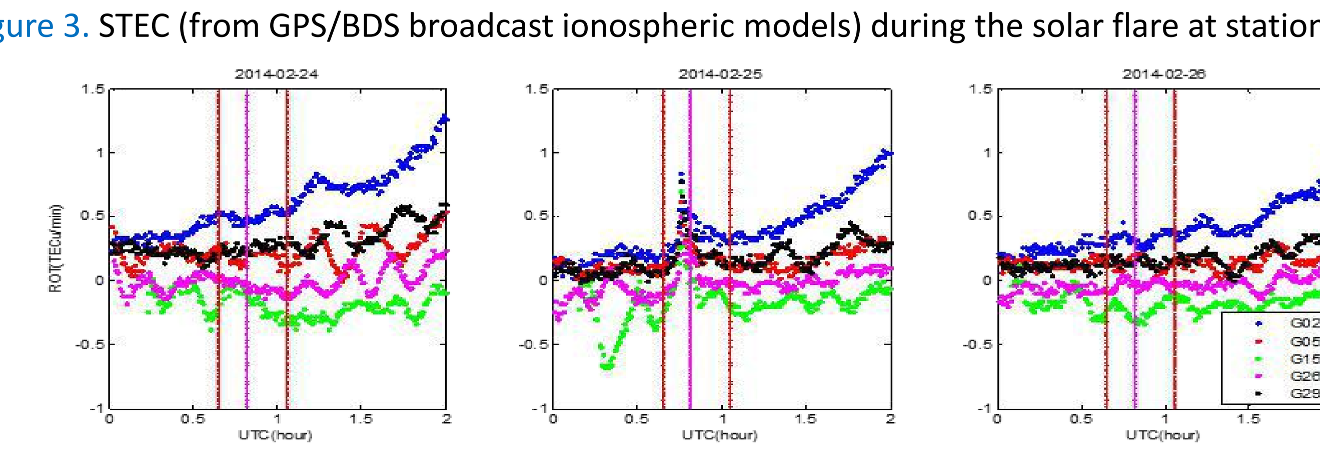

Figure 4. ROT variations during the solar flare at station BJFS

From Figure 2, 3 and 4, we can see that the variations of observed STEC and ROT are obvious with a sudden increase while solar flare occurred. There aren't the same variations for observed STEC and ROT before and after the day when solar flare occurred. Meanwhile, it is found that the STEC calculated with GPS/BDS Klobuchar models remain smoothly and no response to the solar flare.

Table 2. Increment of ROT/STEC/VTEC at stations(TECu)

Pro / Station	dROT			dSTEC			dVTEC		
	24th	25th	26th	24th	25th	26th	24th	25th	26th
BJFS	0.157	0.665	0.131	0.461	2.045	0.836	0.082	0.574	0.849
LHAZ	0.039	0.173	0.078	0.618	1.873	0.082	0.386	0.369	0.315
URUM	0.246	0.180	0.116	1.741	0.556	0.148	0.341	0.155	0.151
WUHN	0.198	0.697	0.185	0.033	1.533	0.875	0.229	0.522	0.225
CHUN	0.135	1.343	0.546	1.373	3.193	0.277	0.334	1.026	0.235
CQCS	0.245	0.607	0.121	0.540	1.843	0.635	0.742	1.186	1.313
DLHA	0.253	0.465	0.210	1.008	1.269	0.864	0.538	0.982	0.788
GSLZ	0.231	0.794	0.213	0.455	1.928	0.945	0.539	0.907	0.694
GUAN	0.129	0.849	0.199	0.127	1.826	0.550	1.174	1.399	0.949
HISY	0.200	0.728	0.099	0.637	1.804	0.668	0.876	0.173	0.245
HLMH	0.142	0.996	0.101	2.824	1.121	1.406	0.637	1.264	0.547
KMIN	0.354	0.586	0.138	0.472	1.916	0.722	0.335	0.580	0.135
SDQD	0.290	1.176	0.262	0.636	2.085	0.772	0.903	0.563	0.081
SHA2	0.266	1.343	0.379	1.147	2.459	0.731	0.219	0.464	0.425
WUSH	0.136	0.169	0.137	0.293	0.685	1.501	0.208	0.239	0.141
XIAA	0.196	0.766	0.237	1.286	2.153	1.317	0.282	0.498	0.789
XZZB	0.092	0.168	0.119	0.336	0.617	0.293	0.383	0.259	0.369

Table 3. Increment of STEC/VTEC during flares(TECu)

Data	Start time（UTC）	End time（UTC）	Class	dSTEC	dVTEC
140225	0039	0103	X4.9	3.19	1.40
141024	2107	2213	X3.1	2.90	1. 35
150505	2205	2215	X2.7	2.64	1.13
150311	1611	1629	X2.2	2.25	1.09
141026	1004	1118	X2.0	2.12	1.13
141022	1402	1450	X1.6	1.57	1.02
141019	0417	0548	X1.1	2.54	1.07
141025	1655	1811	X1.0	2.03	1.04
141022	0116	0228	M8.7	1.32	1.24
150827	0448	0603	M2.9	0.95	0.93
141022	0511	0521	M2.7	0.9	0.91
150621	0102	0200	M2.0	0.89	0.80

From Table 2,we can see that there are large increases of dROT and dSTEC on February 25th than other two days, but it is not so obvious for dVTEC. Moreover, there is a different increment for different stations. We can conclude that there is a Sudden Increase in Total Electron Content (SITEC) caused by solar flares. Table 3 shows the maximum increment of STEC and VTEC during twelve flares.

Effect on accuracy of GPS/BDS Klobuchar model

Table 4. Variations of GPS/BDS dRD at stations(%)

Pro / Station	GPS dRD			BDS dRD		
	24th	25th	26th	24th	25th	26th
BJFS	1.722	5.672	1.723	3.033	4.697	1.892
LHAZ	1.558	7.524	0.806	3.028	3.959	5.653
URUM	2.401	1.740	2.168	2.51	1.827	1.976
WUHN	0.721	3.586	1.725	1.321	3.107	2.287
CHUN	1.419	7.706	0.716	5.487	2.526	0.253
CQCS	0.773	3.972	1.313	5.835	4.093	6.401
DLHA	2.457	4.033	1.990	1.457	1.604	1.018
GSLZ	0.954	7.483	2.315	6.572	1.784	6.313
GUAN	0.665	4.034	1.285	1.009	3.995	2.905
HISY	0.490	3.232	1.386	0.575	4.087	2.562
HLMH	6.285	3.358	3.285	1.84	0.852	0.899
KMIN	1.006	4.748	1.849	2.767	3.563	5.553
SDQD	0.801	7.681	2.138	4.073	5.595	2.718
SHA2	0.875	4.381	1.935	5.443	8.117	6.687
WUSH	3.308	1.211	2.496	0.824	0.425	1.062
XIAA	1.451	5.435	2.709	5.709	3.952	6.601
XZZB	0.596	2.257	0.883	3.084	2.134	1.373

Here a statistical analysis is implemented to calculate the relative difference(RD)between the observed and modeled TEC values for GPS/BDS:

$$RD=\frac{TEC_{mod}-TEC_{obs}}{TEC_{obs}}\times 100\%$$

Table 4 shows the comparison of GPS/BDS dRD （changes of RD） at stations. It can be seen that there are obvious changes of the GPS/BDS ionospheric models accuracy during flares. And the maximum dRD is less than 10% , the dRD on February 25th is larger than other two days. Table 5 shows the maximum variation of GPS/BDS dRD values. There is a certain correlation between the accuracy variation of GPS/BDS ionospheric models and the class of flares.

Table 5. Max variations of GPS/BDS dRD during flares(%)

Data	Start time（UTC）	End time（UTC）	Class	GPS	BDS
140225	0039	0103	X4.9	7.70	8.11
141019	0417	0548	X1.1	3.68	4.66
141022	1402	1450	X1.6	6.07	5.02
141024	2107	2213	X3.1	5.70	4.28
141025	1655	1811	X1.0	3.08	3.16
141026	1004	1118	X2.0	5.06	5.86
150311	1611	1629	X2.2	1.92	1.78
150505	2205	2215	X2.7	5.28	5.41
150621	0102	0200	M2.0	1.53	1.87
150827	0448	0603	M2.9	1.57	1.28
141022	0116	0228	M8.7	2.92	3.30
141022	0511	0521	M2.7	1.15	1.93

Conclusions

- From the observed TEC, it's found that obvious Sudden Increases in Total Electron Content (SITEC) occurred in a short time during solar flares. However, the GPS/BDS broadcast ionospheric models can't reflect the TEC changes .
- The accuracy of GPS/BDS ionospheric models is affected by the SITEC phenomena. The result shows that the variation of relative difference is obvious under solar flares, there is a sudden decrease in RD values.
- The increment of TEC is closely correlated with the maximal X-ray flux during flares. It is also related to the position of stations.

Reference

[1] A Klobuchar J.Ionospheric time delay algorithm for single frequency GPS users [J].IEEETransactions on Eros pace and Electronic Systems, 1987, 23(3):325-331.

[2] Wu Xiaoli, Xiao gong Hu, Gang Wang.Evaluation of COMPASS ionospheric model inGNSS positioning [J]. Advances in Space Research, 2012.

[3] Chen Bin, Liu Libo.A Statistical Analysis of SITEC Caused by Intense Solar Flares during 1996-2003[J]. Chin. J. Space Sci.2005,25(1):6-16.

[4] Afraimovich, E.L., Altyntsev, A.T., Grechnev, V.V., and L. A. Leonovich, Ionospheric effects of the solar flares as deduced from global GPS network data, Adv. Space Res., 27, 1333-1338, 2001c